

E7-2007-86

A. A. Kulko, N. A. Demekhina, R. Kalpakchieva,
N. N. Kolesnikov¹, V. G. Lukashik², Yu. E. Penionzhkevich,
D. N. Rassadov, N. K. Skobelev

ISOMERIC RATIOS FOR $^{196,198}\text{Tl}$ AND $^{196,198}\text{Au}$ FROM
FUSION AND TRANSFER IN THE INTERACTION
OF ^6He WITH ^{197}Au

Submitted to «Journal of Physics G: Nuclear and Particle Physics»

¹Faculty of Physics, Moscow State University, Moscow

²Space Research Institute, RAS, Moscow

Кулько А. А. и др.

E7-2007-86

Изомерные отношения для ядер $^{196,198}\text{Tl}$ и $^{196,198}\text{Au}$, образующихся в реакциях слияния и передачи при взаимодействии ^6He с ^{197}Au

Представлены результаты измерений функций возбуждения и изомерных отношений ядер $^{198\text{m,g}}\text{Tl}$, $^{196\text{m,g}}\text{Tl}$, $^{198\text{m,g}}\text{Au}$ и $^{196\text{m,g}}\text{Au}$, образующихся в реакциях слияния и передачи при взаимодействии ^6He с ядрами ^{197}Au в диапазоне энергий от 5 до 60 МэВ. Вероятность заселения высокоспиновых и низкоспиновых состояний в реакциях слияния–испарения с образованием ядер ^{198}Tl и ^{196}Tl ($J_m^\pi = 7^+$, $J_g^\pi = 2^-$), а также в реакциях передачи с образованием ядер ^{198}Au и ^{196}Au ($J_m^\pi = 12^-$, $J_g^\pi = 2^-$) сравнивается с расчетными данными в рамках статистической модели, а также с результатами измерений на пучках дейтронов.

Работа выполнена в Лаборатории ядерных реакций им. Г. Н. Флерова ОИЯИ.

Препринт Объединенного института ядерных исследований. Дубна, 2007

Kulko A. A. et al.

E7-2007-86

Isomeric Ratios for $^{196,198}\text{Tl}$ and $^{196,198}\text{Au}$ from Fusion and Transfer in the Interaction of ^6He with ^{197}Au

Excitation functions and isomeric cross-section ratios have been measured for the nuclei $^{198\text{m,g}}\text{Tl}$, $^{196\text{m,g}}\text{Tl}$, $^{198\text{m,g}}\text{Au}$ and $^{196\text{m,g}}\text{Au}$, formed in fusion–evaporation and transfer processes in reactions of ^6He with ^{197}Au in the energy range 5–60 MeV. The population probability of high- and low-spin states in the fusion reaction with the formation of ^{198}Tl and ^{196}Tl ($J_m^\pi = 7^+$, $J_g^\pi = 2^-$), as well as of the transfer products ^{198}Au and ^{196}Au ($J_m^\pi = 12^-$, $J_g^\pi = 2^-$), is compared with calculations within the statistical model and with similar results from deuteron-induced reactions.

The investigation has been performed at the Flerov Laboratory of Nuclear Reactions, JINR.

Preprint of the Joint Institute for Nuclear Research. Dubna, 2007

INTRODUCTION

The population of the ground and metastable states of nuclei, formed as reaction products, strongly depends on the acquired excitation energy of the residual nucleus, its angular momentum distribution and on the type of particles emitted during its de-excitation. The relative population of the ground and metastable states depends on the orbital angular momentum ℓ in the entrance channel of the reaction. The emitted particles carry away different amount of energy and angular momentum. The comparison of the measured isomeric cross-section ratios σ_m/σ_g , where σ_m is the cross section for populating the metastable state of a nucleus and σ_g — that for populating its ground state, with calculations within different models [1–7] helps to estimate the spin associated with the reaction products, produced in different exit channels. Hence, isomeric ratios deduced in different nuclear reactions in a wide range of incident projectile energies provide important information on the structure of a nucleus and on the mechanism of its production, in particular on the distribution of the nuclear level density and on the spin of the excited levels of the precursor.

There are different methods to determine isomeric cross-section ratios: *on-line* measurement of the decay from the ground and metastable states of the studied nucleus [8] or *off-line* measurement of the yield of these states after accumulation in a nuclear reaction. The first of these methods allows a detailed studying of the structure of the ground and metastable states during the process of their production, but it is not efficient enough. In the second method, the final products are accumulated using the maximum possible beam intensities, and consequently, it is characterized by high efficiency. However, it is sometimes rather complicated to determine the cross sections of the reaction products, because of the cumulativity of their production. This method is preferable in cases when radioactive beams of low intensity are used, and hence — highest efficiency is needed. These requirements are met by the stack activation technique, which we have already used in our experiments aimed to study the interaction of ${}^6\text{He}$ with ${}^{197}\text{Au}$ [9, 10].

At present, there is much interest in the investigation of reactions induced by weakly bound radioactive nuclei with unusual nucleon distributions, which strongly influence the interaction process [9, 10 and ref. therein]. In the case

of reactions induced by ${}^6\text{He}$ (a nucleus with a neutron skin), one can expect, as a result of the greater mass of ${}^6\text{He}$ and its larger matter radius, an increase in the admitted average angular momentum compared to reactions with ${}^4\text{He}$. It is probable that the interaction of ${}^6\text{He}$ brings forth in the residual nuclei a wider angular momentum distribution and a higher average angular momentum. This distribution, in turn, may affect the relative population of the metastable and ground states in the evaporation residues compared to the case of fusion reactions induced by normal stable nuclei, such as α particles, ${}^6\text{Li}$, etc.

Although much experimental and theoretical effort [10 and ref. therein] has been devoted to study how the structure of radioactive nuclei influences the fusion process at energies close to the Coulomb barrier, the data on the population of high-spin states in reactions induced by exotic nuclei are rather scarce [8].

The main factors which govern the isomeric ratios are: 1) the distribution of excitation energy and angular momentum in the compound nuclei, 2) the number of de-excitation cascades and decay paths of each state, 3) the angular momentum removed by the emitted particle or γ quantum at each step of the de-excitation, 4) the probability of population of the ground and metastable states after each step of the de-excitation cascade, and 5) the spins of the isomeric-pair states.

When the projectile energy is high enough to populate states with different angular momenta, the isomeric cross-section ratio tends to the limiting value of $(2J_m + 1)/(2J_g + 1)$ defined as the «statistical weight». In calculating the isomeric ratios for transfer products some assumptions have to be made for the energy and the angular momentum of the transferred particle. When a low-energy particle with a small angular momentum is transferred, the process of particle evaporation will be suppressed and the number of steps in the γ cascade will be reduced.

The aim of the present work was to study the fusion of the loosely bound nuclei ${}^6\text{He}$ with ${}^{197}\text{Au}$ leading to the formation of the compound nucleus ${}^{203}\text{Tl}$. For this purpose the population of the ground and metastable states of the residual nuclei ${}^{198}\text{Tl}$ and ${}^{196}\text{Tl}$, produced in the reaction ${}^{197}\text{Au}({}^6\text{He}, xn){}^{203-xn}\text{Tl}$, where $x = 5$ and 7 , was measured. The transfer reactions leading to the isotopes ${}^{196}\text{Au}$ and ${}^{198}\text{Au}$ were also studied. A comparison of the isomeric ratios of these nuclei, produced in reactions induced by ${}^6\text{He}$ and α particles will make it possible to draw conclusions about the maximum imported angular momentum and the probability of population of high-spin states in the residual Tl (7^+ in ${}^{198\text{m}}\text{Tl}$ and ${}^{196\text{m}}\text{Tl}$) and Au (12^- in ${}^{196\text{m}}\text{Au}$ and ${}^{198\text{m}}\text{Au}$) isotopes.

1. EXPERIMENT

The ${}^6\text{He}$ beam was produced at the accelerator complex for radioactive nuclei DRIBs at FLNR, JINR. This complex is a tandem including the cyclotrons U400

and U400M [11]. The maximum energy of the accelerated ${}^6\text{He}$ ions was about 10 MeV/A, the intensity reaching $2 \cdot 10^7$ pps [9, 10].

The yields of the fusion reaction evaporation residues and of the transfer reactions were performed by the stacked foil activation technique [9, 10]. The stack, consisting of gold foils of different thickness (from 13.5 to 50 μm), was placed in the scattering chamber in front of the magnetic spectrometer MSP-144 [12], which was used to measure the initial and residual energy of the beam (after passing the target stack), as well as the energy incident on each successive target (or, what is the same — the energy exiting the previous one) by inserting the targets into the stack one after another. The ${}^6\text{He}$ -beam energy at each cross-section point was taken as the average of the ion energy upon entering and exiting the respective target foil, while the corresponding energy spread was determined mainly by the energy loss of the beam particles in that foil. In addition, the ${}^6\text{He}$ energy and energy loss for each layer in the stack were calculated using the code LISE [13] and then compared with the measured values. The given technique made it possible to measure the excitation functions for the production of the Tl and Au isotopes in a wide energy range. A detailed description of the experiments can be found in [9, 10].

2. ANALYSIS OF THE EXPERIMENTAL DATA

After each irradiation (the data were taken in four different runs), the γ activity, induced in the individual gold foils, was measured *off-line* using four HPGe detectors. The energy resolution for the transition $E_\gamma = 662$ keV was 1.2 keV and the efficiency reached $\sim 5\%$ for different detectors. For the analysis of the γ spectra, the program DEIMOS-32 was used [14]. The identification of the radioactive residues from the interaction of ${}^6\text{He}$ with ${}^{197}\text{Au}$ was performed according to the γ -transition energies and the half-lives of the Tl isotopes (for the fusion evaporation reaction) and of the Au isotopes (for the transfer reaction). The decay data (energies, absolute intensities and half-lives) taken from [15], used for identification and determining the yields of the Tl and Au isotopes, are given in Table 1.

A typical γ spectrum, measured during 0.5 h about 2 h after the irradiation of one of the gold targets, is shown in Fig. 1. The absolute cross sections for the formation of the reaction products were calculated taking into account the relevant beam dose and time factors, the target thickness and the decay characteristics of the identified isotopes using the formula:

$$\sigma = \frac{S \cdot \lambda}{I \cdot N \cdot \varepsilon \cdot I_\gamma \cdot (1 - e^{-\lambda \cdot t_1}) \cdot e^{-\lambda \cdot t_2} \cdot (1 - e^{-\lambda \cdot t_3})}, \quad (1)$$

where S is the number of counts in the photopeak for the time of γ -spectrum

Table 1. Spectroscopic data [15] for the studied reaction products $^{196,198}\text{Tl}$ and $^{196,198}\text{Au}$ in their ground and metastable states

| Residual nucleus | $T_{1/2}$ | J^π | E_γ (keV) | I_γ (%) |
|----------------------------|-----------|---------|------------------|----------------|
| $^{196\text{g}}\text{Tl}$ | 1.84 h | 2^- | 344.9 | 2 |
| $^{196\text{m}}\text{Tl}$ | 1.41 h | 7^+ | 505.2 | 6 |
| | | | 695.6 | 41 |
| $^{198\text{g}}\text{Tl}$ | 5.3 h | 2^- | 675.9 | 11 |
| $^{198\text{m}}\text{Tl}$ | 1.87 h | 7^+ | 587.2 | 52 |
| $^{196\text{g}}\text{Au}$ | 6.183 d | 2^- | 332.983 | 22.9 |
| | | | 355.684 | 87 |
| | | | 426.0 | 7 |
| $^{196\text{m}2}\text{Au}$ | 9.6 h | 12^- | 147.81 | 43 |
| | | | 168.37 | 7.6 |
| | | | 188.27 | 37.4 |
| $^{198\text{g}}\text{Au}$ | 2.69 d | 2^- | 411.8 | 96 |
| $^{198\text{m}}\text{Au}$ | 2.27 d | 12^- | 180.31 | 50 |
| | | | 204.10 | 40.8 |
| | | | 214.84 | 77 |

measurement t_3 , λ — the decay constant of a given isotope, t_2 — the time elapsed between the end of irradiation and the start of the γ -activity measurement, t_1 — the time of irradiation, N — the target thickness in atoms/cm², I — the beam intensity in unit time (pps), I_γ — the absolute intensity of the given γ transition (%), and ε — the γ -detector efficiency for the given γ line.

The isotopes ^{198}Tl , ^{196}Tl , ^{198}Au and ^{196}Au were identified both in their ground and metastable states. If the decay of the metastable state leads to population of the ground state, the independent yield of the latter is calculated by taking into account the contribution of the precursor (the isomer) by means of the formula:

$$\sigma_d = \frac{\left(\frac{S}{I \cdot N \cdot \varepsilon \cdot I_\gamma} - k_{\text{br}} \cdot \sigma_p \cdot A \right) \lambda_d}{(1 - e^{-\lambda_d t_1}) \cdot e^{-\lambda_d t_2} \cdot (1 - e^{-\lambda_d t_3})} \quad , \quad (2)$$

$$A = \frac{\lambda_p \cdot \lambda_d}{\lambda_d - \lambda_p} \times \left[\frac{(1 - e^{-\lambda_p t_1})}{\lambda_p^2} \cdot e^{-\lambda_p t_2} \cdot (1 - e^{-\lambda_p t_3}) - \frac{(1 - e^{-\lambda_d t_1})}{\lambda_d^2} \cdot e^{-\lambda_d t_2} \cdot (1 - e^{-\lambda_d t_3}) \right] ,$$

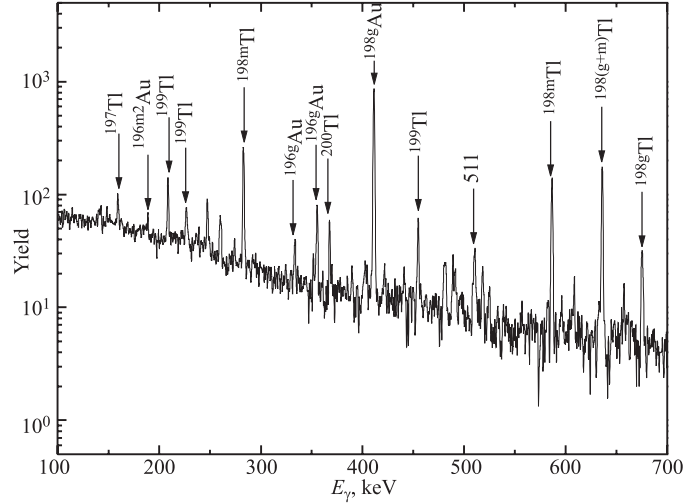


Fig. 1. A typical *off-line* γ spectrum for one gold target, measured about 2 h after the irradiation with a 40-MeV ${}^6\text{He}$ beam; g and m denote γ transitions from the ground and metastable states, respectively

where σ_p , σ_d are the cross sections for formation of the parent (the metastable) and the daughter (the ground) states, respectively; λ_p , λ_d are their decay constants, k_{br} — the branching ratio in the given decay scheme.

Since the isomeric ratios are determined by the ratio of the cross sections for populating the metastable and the ground states of a nuclide in a nuclear reaction, the main contribution to the error comes from statistical errors in calculating the number of counts in the photopeaks.

3. EXPERIMENTAL RESULTS AND DISCUSSION

In the reaction ${}^{197}\text{Au}({}^6\text{He}, 5n){}^{198}\text{Tl}$, both the ground (${}^{198g}\text{Tl}$) and the metastable state (${}^{198m}\text{Tl}$) are populated. The energy dependence of the respective production cross sections is shown in Fig. 2, *a*, together with the isomeric ratio σ_m/σ_g in Fig. 2, *b*. The isomeric ratio σ_m/σ_g for ${}^{196}\text{Tl}$ was also measured, but only at two energies higher than 50 MeV (see Table 2): the deduced values are almost equal and are close to the maximum value of σ_m/σ_g , obtained for ${}^{198}\text{Tl}$. It is noteworthy that the experimental isomeric ratios for ${}^{198,196}\text{Tl}$ are somewhat smaller than the values following from the relation $(2J_m + 1)/(2J_g + 1)$.

The calculations of the isomeric ratio for ${}^{198m,g}\text{Tl}$, performed within the statistical model, are shown in Fig. 2, *b*. It is assumed that the reaction proceeds

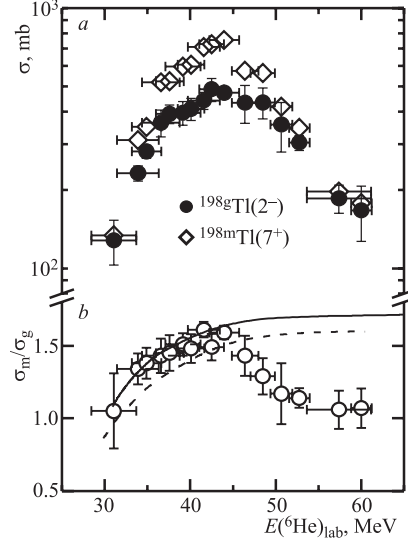


Fig. 2. *a*) Experimental excitation functions for the $^{197}\text{Au}(^6\text{He}, 5n)^{198}\text{Tl}$ reaction: \bullet — ground state (2^-), \diamond — metastable state (7^+); *b*) isomeric ratio for nucleus ^{198}Tl . The lines denote calculations within the statistical model using the density level parameter $a = 20 \text{ MeV}^{-1}$ and two values of the spin-cutoff parameter σ_0 : 5.3 (solid line) and 5 (dashed line), respectively [16]

Table 2. Experimental cross sections σ_m , σ_g , and the isomeric ratio (σ_m/σ_g) for the ^{196}Tl nucleus, produced in the $^{197}\text{Au}(^6\text{He}, 7n)$ reaction at 60 and 57.4 MeV

| $E_{\text{lab}}, \text{ MeV}$ | $\sigma_m, \text{ mb}$ | $\sigma_g, \text{ mb}$ | σ_m/σ_g |
|-------------------------------|------------------------|------------------------|---------------------|
| 60 ± 1.2 | 549 ± 66 | 292 ± 65 | 1.88 ± 0.18 |
| 57.4 ± 3.7 | 465 ± 9 | 251 ± 55 | 1.85 ± 0.13 |

in the same way as it has been described in [1]. The usual relations for the excitation energy dependence of the level density parameter (a) and of the angular momentum (ℓ) were applied [16]. The value of the level density parameter was fixed, while the spin-cutoff parameter σ_0 was varied, so as to obtain the best agreement with the experimental isomeric ratios. It is seen from the figure that for ^{198}Tl for incident energies up to 45 MeV the experimental and calculated values of σ_m/σ_g practically coincide and increase until they reach a maximum. The value $\sigma_0 = 5.3$ better fits the data. The increase with bombarding energy is expected since higher ℓ waves are involved and the average spin of the compound

nucleus increases. With the further increase of the projectile energy (above 45–50 MeV), the experimental σ_m/σ_g ratio decreases, strongly differing from the theoretical calculations, but remains larger than 1 in the used energy range. This behaviour may be due to the opening of competing reactions, including the $6n$ -evaporation channel and pre-equilibrium processes, accompanied by neutron emission. The emission of neutrons, before equilibrium is attained, has been observed as retardation of the «tails» of the excitation functions at high energies [10 and ref. therein]. In Refs. [17, 20] the decrease of the isomeric ratio with the increase of the projectile energy has been attributed to the probability of pre-equilibrium processes.

The isomeric ratio for $^{198m.g}\text{Tl}$, obtained in different α -particle-induced reactions [17–19], varies from 1 to 5. For this reason it is impossible to draw unambiguous comparative conclusions with respect to the present data. Nevertheless, from our data on the isomeric ratios for the nuclei $^{198m.g}\text{Tl}$, produced in the fusion of ^6He with ^{198}Au , it follows that the population of metastable states in this reaction (in spite of the higher excitation energy of the compound nucleus) is of the same order of magnitude as in the case of α -particle-induced reactions [17–19].

The data that we have obtained confirm the conclusions made in [8]. Here, the isomeric ratio for the $3n$ -evaporation exit channel $^{209}\text{Bi}(^6\text{He}, 3n)^{212m.g}\text{At}$ ($J^\pi = 9^-$ and $J^\pi = 1^-$) was measured and an increase in the isomeric ratio with increasing energy of the ^6He projectile was observed. Its value was in agreement with standard calculations and in the maximum of the excitation function it was lower than the limit defined by the statistical weight.

The isomeric ratios strongly depend on the transferred orbital angular momentum, while the dependence on the number of evaporated neutrons by the compound nucleus is rather weak [7]. In the range of the incident ^6He energies used in the present experiments, the best agreement between the calculated and experimental isomeric ratios for the ^{196}Tl and ^{198}Tl nuclei was obtained for average imported angular momenta between 5 and 22 η (depending on the incident energy). It has been shown in [7, 8, 17] that the same values are reached in experiments with ^3He , ^4He and ^6He beams.

The cross sections for producing ^{198}Au in the metastable and ground (^{198m}Au and ^{198g}Au) states in the $^6\text{He} + ^{197}\text{Au}$ reaction as a function of difference between the incident energy and the Coulomb barrier, $E_{\text{cm}} - B_c$, in the c.m.-system, are shown in Fig. 3. The shape of the excitation function of ^{198}Au provides evidence that ^{198m}Au and ^{198g}Au are produced in direct reactions as transfer products; for this reason it is not possible to interpret them using the statistical model. In the same figure, the excitation functions for the formation of ^{198}Au in the ground and metastable states in deuteron-induced reactions [21–23] are plotted for comparison. It can be seen that the two reactions leading to ^{198}Au have their maxima at the Coulomb barrier. However, the cross section in the case

of the ${}^6\text{He}$ beam is much higher. This can be due to the fact that the neutron separation energy for ${}^6\text{He}$ is much lower than for the deuteron.

The isomeric ratio for the isotope ${}^{198}\text{Au}$, together with the corresponding cross sections of its production in the ground and metastable states, are shown in Fig. 4. As can be seen from the figure, the production of the isomer compared to that of the ground state is less probable. This may be due to the fact that one neutron transferred to the target nucleus brings in a comparatively low angular momentum, and thus considerably decreases the probability of populating the metastable state (12^-) in the ${}^{198}\text{Au}$ nucleus. It can be seen from the presented data on the cross section of fusion–evaporation and transfer reactions measured with deuteron and ${}^6\text{He}$ beams, that the positions of the maxima of the excitation functions for the ground and metastable states differ. As a rule (see, for example, [1, 7]), the excitation function for the metastable state peaks at higher incident energy compared to that of the ground state.

The dependence on $(E_{\text{cm}} - B_c)$ of the isomeric ratios for ${}^{198}\text{Au}$, $\sigma({}^{198\text{m}}\text{Au})/\sigma({}^{198\text{g}}\text{Au})$, obtained in reactions with deuteron and ${}^6\text{He}$ beams, is presented in Fig. 5. In the case of the ${}^6\text{He}$ -induced reaction, the dependence extends further down below the barrier region.

The excitation functions for the ground and metastable states of ${}^{196}\text{Au}$, produced after one-neutron stripping in the ${}^6\text{He} + {}^{197}\text{Au}$ reaction, are given in Fig. 6.

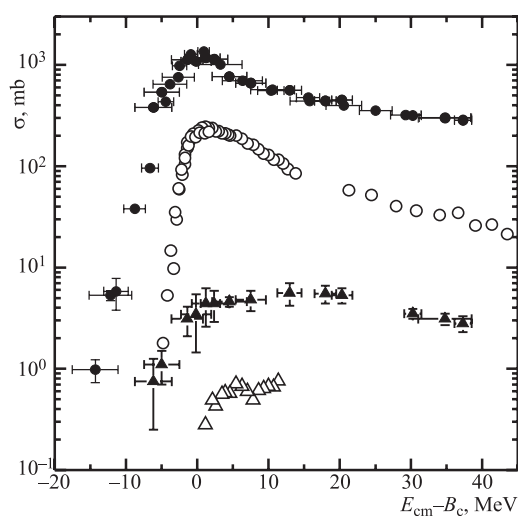


Fig. 3. Excitation functions for one-neutron transfer in the reactions ${}^6\text{He} + {}^{197}\text{Au}$, leading to formation of isotope ${}^{198}\text{Au}$ in the ground and metastable states (\bullet — ${}^{198\text{g}}\text{Au}$, \blacktriangle — ${}^{198\text{m}}\text{Au}$), as a function of difference between the incident energy and the Coulomb barrier, $E_{\text{cm}} - B_c$, in the c.m.-system [10]. Data for ${}^{198}\text{Au}$ from the ${}^{197}\text{Au} + d$ reaction (\circ — ${}^{198\text{g}}\text{Au}$, Δ — ${}^{198\text{m}}\text{Au}$) are plotted for comparison [21–23]

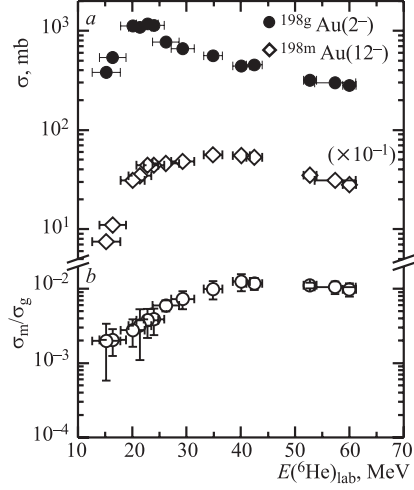


Fig. 4. *a*) Excitation functions for one-neutron transfer through the reaction ${}^6\text{He} + {}^{197}\text{Au}$, producing ${}^{198}\text{Au}$ in the ground 2^- (\bullet) and in the metastable 12^- (\diamond) states; *b*) associated isomeric ratios (\circ) for ${}^{198}\text{Au}$

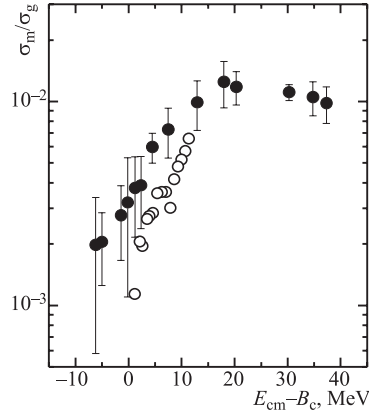


Fig. 5. Measured isomeric ratios for nucleus ${}^{198}\text{Au}$, formed in the reactions: ${}^6\text{He} + {}^{197}\text{Au}$ — present work (\bullet), and ${}^{197}\text{Au} + d$ — [22] (\circ), as a function of difference $E_{\text{cm}} - B_c$

The associated isomeric ratios are shown in the lower part of the figure. In this reaction, in the used energy range, the isomeric ratio changes weakly. However, its value is higher than in the case of ${}^{198}\text{Au}$. Obviously, this is connected with the transferred angular momentum: when the ${}^6\text{He}$ projectile knocks out a neutron from the target nucleus the transferred angular momentum is higher than

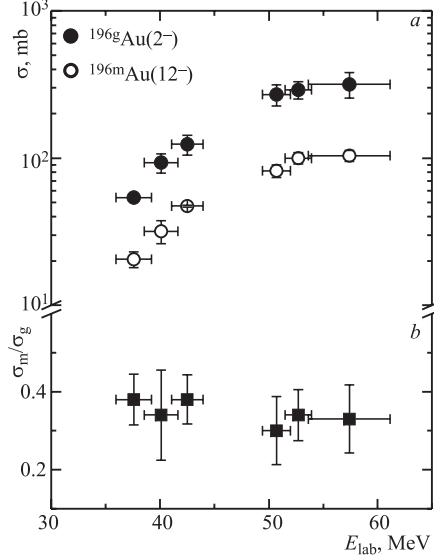


Fig. 6. *a)* Excitation functions for one-neutron removal in the interaction of ${}^6\text{He}$ with ${}^{197}\text{Au}$, leading to the ground 2^- state (\bullet) and to the metastable 12^- state (\circ) in ${}^{196}\text{Au}$; *b)* corresponding isomeric ratios (\blacksquare) for the ${}^{196}\text{Au}$ nucleus

when a neutron is added. During the collision of ${}^6\text{He}$ with the ${}^{197}\text{Au}$ nucleus, a large amount of energy and momentum is transferred, which, in turn, leads to the escape of a neutron from the target nucleus and increases the probability of populating the metastable state in the residual excited ${}^{196}\text{Au}$ nucleus.

Summarizing our results, we should point to the following:

- Isomeric ratios have been measured for fusion–evaporation products (${}^{196,198}\text{Tl}$) and for transfer products (${}^{196,198}\text{Au}$), produced in ${}^6\text{He}$ -induced reactions.
- The isomeric ratios for ${}^{196,198}\text{Tl}$, produced in the ${}^6\text{He} + {}^{197}\text{Au}$ reaction, are close in absolute value to those obtained in ${}^4\text{He}$ -induced reactions.
- The isomeric ratios for fusion reactions followed by the evaporation of 5 to 7 neutrons exceed by 1–3 orders of magnitude the ratios obtained for neutron transfer products.
- In the case of transfer reactions, the isomeric ratios for ${}^{196}\text{Au}$ and ${}^{198}\text{Au}$ show different incident energy dependence and differ in absolute value: in the case of neutron removal from ${}^{197}\text{Au}$ the isomeric ratios are higher than for the transfer of a neutron to ${}^{197}\text{Au}$.

Acknowledgements. The authors are indebted to the members of the FLNR Accelerator staff for the stable operation of the DRIBs complex and the high quality of the ^6He beam. We also gratefully acknowledge the fruitful discussions with T. V. Chuvilskaya and Yu. A. Muzychka. The present work was performed with the partial support by Grants of the RFBR 05-02-19813-MF-a and 07-02-00251-a.

REFERENCES

1. *Huizenga J. R., Vandebosch R.* // Phys. Rev. 1960. V. 120. P. 1305, 1313.
2. *Bishop C. T., Huizenga J. R., Hummel J. P.* // Phys. Rev. 1964. V. 135. P. B401.
3. *Qaim S. M., Mushtaq A., Uhl M.* // Phys. Rev. C. 1988. V. 38. P. 645.
4. *Cserpak F. et al.* // Phys. Rev. C. 1994. V. 49. P. 1525.
5. *Vishnevski I. N., Zheltonozhski V. A., Lashko T. N.* // Yad. Fiz. 1985. V. 41. P. 1435.
6. *Nagame Y., Nakamura Y. et al.* // Nucl. Phys. A. 1988. V. 486. P. 77.
7. *Nagame Y. et al.* // Phys. Rev. C. 1990. V. 41. P. 889.
8. *de Young P. A. et al.* // Phys. Rev. C. 2000. V. 62. P. 047601.
9. *Penionzhkevich Yu. E. et al.* // Part. & Nucl., Lett. 2006. V. 3, № 6. P. 38.
10. *Penionzhkevich Yu. E. et al.* // Eur. Phys. J. A. 2007. V. 31. P. 185.
11. *Oganessian Yu. Ts., Gulbekian G. G.* // Proc. of the Int. Conf. «Nuclear Shells — 50 Years», Dubna, Russia, 1999 / Eds. Oganessian Yu. Ts., von Oertzen W., Kalpakchieva R. Singapore: World Scientific, 2000. P. 61–75.
12. *Skobelev N. K. et al.* // Nucl. Instr. and Meth. B. 2005. V. 227. P. 471.
13. <http://dnr080.jinr.ru/lise/>; <http://groups.nsl.msu.edu/lise/>
14. *Frama J.* // Radioanalyt. and Nucl. Chem. 2003. V. 257. P. 583.
15. <http://nucleardata.nuclear.lu.se/NuclearData/toi/>
16. *Kolesnikov N. N., Gubin V. B.* // Izv. Vuzov MV SSSR, Physics. 1984. № 8. P. 77 (in Russian).
17. *Chakravarty N., Sarkar P. K., Ghosh Sudip* // Phys. Rev. C. 1992. V. 45. P. 1171.
18. *Lanzaforame F. M., Blann M.* // Nucl. Phys. A. 1970. V. 142. P. 545.
19. *Capurro O. A., de la Vega Vedoya M., Nassiff S. J.* // J. Radioanalyt. and Nucl. Chem. Lett. 1985. V. 128. P. 403.
20. *Bissem H. H. et al.* // Phys. Rev. C. 1980. V. 22. P. 1468.
21. *Long X. et al.* // Inst. of Nucl. Sci. and Technol. 1985. Reports No. 001.
22. *Casella V. R.* // Report UC-34 c, (LA-5830-T). 1975.
23. *Jahn P., Probst H.-J. et al.* // Nucl. Phys. A. 1973. V. 209. P. 333.

Received on June 13, 2007.

Редактор *В. В. Булатова*

Подписано в печать 24.12.2007.

Формат 60 × 90/16. Бумага офсетная. Печать офсетная.

Усл. печ. л. 0,87. Уч.-изд. л. 1,2. Тираж 300 экз. Заказ № 56007.

Издательский отдел Объединенного института ядерных исследований
141980, г. Дубна, Московская обл., ул. Жолио-Кюри, 6.

E-mail: publish@jinr.ru

www.jinr.ru/publish/